

Electronic Supplementary Information for:
Permanently Porous Hydrogen-Bonded Frameworks of
Rod-like Thiophenes, Selenophenes, and Tellurophenes
Capped with MIDA Boronates

Peng-Fei Li, Chenxi Qian, Alan J. Lough, Geoffrey A. Ozin, and Dwight S. Seferos*

Department of Chemistry, University of Toronto 80 St. George, Toronto, ON M5S 3H6

(Canada). E-mail: dseferos@chem.utoronto.ca

Table of Contents

General methods and materials.....	3
General procedure for boronate synthesis.....	3
Instrumentation.....	4
Absolute Quantum Yield Measurement.....	5
Figure S1-S3. FT-IR spectra.....	6
Figure S4. Hydrogen-bonding interactions in the single crystal of DPSe-MIDA	7
Figure S5. Microporous structure of DPT-MIDA	7
Figure S6-S7. Interaction between guest and DPT-MIDA , DPSe-MIDA	8
Figure S8-S9. Comparison of experimental and simulated PXRD patterns.....	9
Figure S10. PXRD patterns comparison of three frameworks.....	10
Figure S11-S13. TGA of three frameworks.....	10-11
Figure S14-S19. NMR spectra.....	12-14
Figure S20-S21. Variable temperature PXRD patterns under air.....	15
Figure S22. Variable temperature PXRD patterns under vacuum.....	16
Figure S23. PXRD patterns of blank dome.....	16
Figure S24. Optical microscope images of DPSe-MIDA	17
Figure S25. Linear relationship of BET surface area and Mn.....	17
Figure S26-S28. Pore distribution of three frameworks.....	18-19
Figure S29. Normalized UV-Vis of boronate in solution.....	19

Figure S30. Fluorescence spectra of boronate in solution.....	20
Figure S31. Image of DPT-MIDA powder excited by a UV lamp at 365 nm.....	20
Table S1-S2. Crystal data and structure refinement.....	21-22

General methods and materials: All reagents were used as received unless otherwise noted. 4-Iodophenylboronic acid MIDA ester, and Tetrakis(triphenylphosphine)palladium were purchased from Sigma-Aldrich. Copper(I) iodide were purchased from Alfa Aesar. All reactions were carried out under argon using oven-dried glassware. TLC was performed on silica gel GF₂₅₄; chromatograms were visualized with UV light (254 and 360 nm). Flash column chromatography was performed on 200-300 mesh silica gel. The synthesis of 2,5-bis(trimethyltin)thiophene, 2,5-bis(trimethyltin)selenophene, and 2,5-bis(trimethyltin)tellurophene was performed according to literature methods (references in the main text).

General procedure for DPT-, DPSe-, and DPTe-MIDA boronate synthesis:

A 100 mL Schlenk flask was charged with 4-Iodophenylboronic acid MIDA ester (1.31 g, 3.6 mmol), 2, 5-Bis(trimethyltin)thiophene (0.5 g, 1.2 mmol), Copper(I) iodide (46 mg, 0.02 mmol) and Tetrakis(triphenylphosphine)palladium (282 mg, 0.02 mmol) under argon. Dry degassed DMF (50 mL) was added through a syringe to afford a yellow solution. After stirring at r.t. for 10 min, the mixture was heated to 100 °C under argon overnight. After cooling to r.t., the mixture was filtered and concentrated under vacuum. The crude product was stirred with a small amount of acetonitrile and filtered. The resultant solid was recrystallized in acetonitrile to afford a light yellow solid.

DPT-MIDA

Yellow solid, m.p. >300 °C, yield: 90 %. IR with ATR: 1746(s), 1219(s), 1037(s), 986(s), 797(s) cm⁻¹. ¹H NMR (400 MHz, DMSO-*d*₆) δ 7.69 (d, *J* = 8.3 Hz, 4H), 7.59 (s, 2H), 7.49 (d, *J* = 8.3 Hz, 4H), 4.35 (d, *J* = 17.2 Hz, 4H), 4.13 (d, *J* = 17.2 Hz, 4H), 2.54 (s, 6H). ¹³C NMR (100 MHz, DMSO-*d*₆) δ 169.35, 142.65, 133.84, 133.21, 125.00, 124.38, 61.79, 47.58, 39.52. ESI-HRMS mass for C₂₆H₂₅B₂N₂O₈S [M+H]⁺: calculated 547.1522, measured 547.1517.

DPSe-MIDA

Yellow solid, m.p. >300 °C, yield: 87 %. IR with ATR: 1743(s), 1602(w), 1456(w), 1289(w), 1232(w), 1019(w), 995(s), 798(s) cm⁻¹. ¹H NMR (400 MHz, DMSO-*d*₆) δ 7.73 (s, 2H), 7.64 (d, *J* = 8.2 Hz, 4H), 7.48 (d, *J* = 8.2 Hz, 4H), 4.35 (d, *J* = 17.2 Hz, 4H), 4.13 (d, *J* = 17.2 Hz, 4H), 2.54 (s, 6H). ¹³C NMR (100 MHz, DMSO-*d*₆) δ 169.37, 148.82, 135.85, 133.25, 127.08, 124.84, 61.79, 47.58. ESI-HRMS mass for C₂₆H₂₅B₂N₂O₈Se [M+H]⁺: calculated 595.0962, measured 595.0961.

DPTe-MIDA

Yellow solid, m.p. >300 °C, yield: 84 %. IR with ATR: 3006(w), 1738(s), 1598(w), 1454(w), 1290(s), 1218(s), 982(s), 801(s) cm⁻¹. ¹H NMR (400 MHz, DMSO-*d*₆) δ 8.08 (s, 2H), 7.59-7.53 (m, 4H), 7.47-7.39 (m, 4H), 4.35 (d, *J* = 17.2 Hz, 4H), 4.12 (d, *J* = 17.2 Hz, 4H), 2.54 (s, 6H). ¹³C NMR (100 MHz, DMSO-*d*₆) δ 169.41, 147.71, 139.57, 134.50, 133.26, 125.70, 61.80, 47.60. ESI-HRMS mass for C₂₆H₂₅B₂N₂O₈Te [M+H]⁺: calculated 645.0865, measured 645.0862.

Instrumentation

NMR spectra were recorded on a Varian Mercury 400 spectrometer (400 MHz). Fourier transform infrared spectroscopy (FT-IR) was measured using a Perkin Elmer Spectrum BX with ATR accessory. Thermogravimetric analysis was measured on a TA Instruments SDT-Q600 Thermo Gravimetric analyzer at a heating rate of 10°C/min under a nitrogen gas flow of 100 mL/min on an alumina pan. Powder diffraction data were obtained using a Bruker D8 Davinci with focused Co radiation and a Vantec 500 area detector. The samples were covered with a polyether ether ketone polymer dome to protect the detector. Microscope images were taken on an Axio Imager A2m. Absorption spectra were recorded using a Varian Cary 5000 spectrometer. Fluorescence spectra were recorded using a Photon Technology International (PTI) QuantaMaster 40-F NA spectrofluorometer with a xenon arc light source and 914 Photomultiplier Detection System. CO₂ adsorption isotherms were performed at Quantachrome's Material Characterization Laboratory using an Autosorb Station 2.

Absolute Quantum Yield Measurement

The absolute quantum yield was determined using a previously reported integrating sphere method.^{1,2} Samples were excited in an integrating sphere (Gigahertz Optik, custom made) with light from a 365nm LED (Thorlabs M365L2), and photoluminescence was collected by a 1 mm diameter optical fibre (Ocean Optics) and detected by an Ocean Optics Maya 2000 spectrometer. The continuous absolute quantum yield was measured by taking appropriate ratios of the excitation and emission peak areas of spectra recorded for the empty sphere and sample holder, and the excitation focused directly onto the sample. The accuracy of the system was verified against literature values for rhodamine 6G and MEH-PPV. Film samples were sealed in a custom made sample holder.

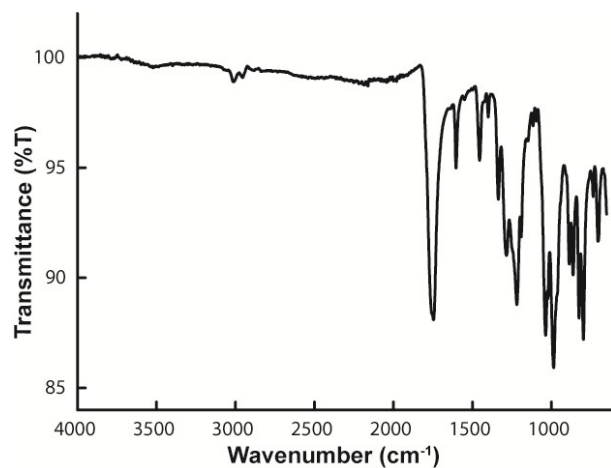


Figure S1. IR spectrum of **DPT-MIDA**.

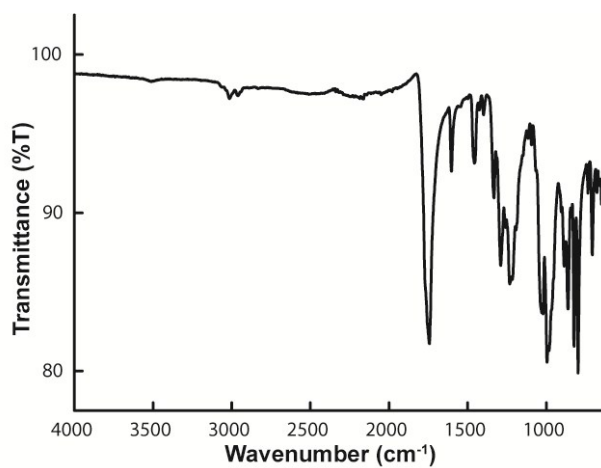


Figure S2. IR spectrum of **DPSe-MIDA**.

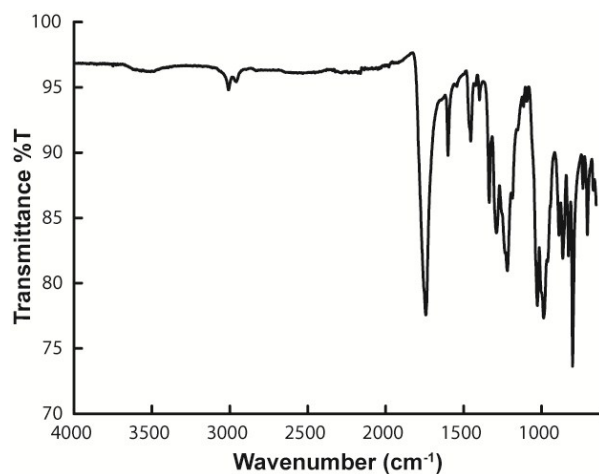


Figure S3. IR spectrum of **DPTe-MIDA**.

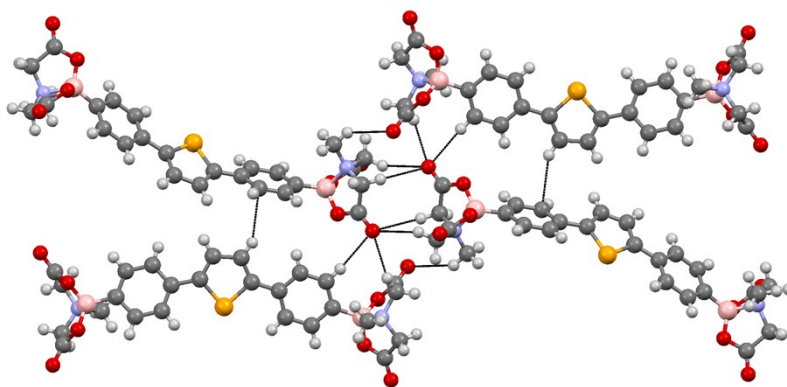


Figure S4. Hydrogen-bonding interactions in the single crystal of **DPSe-MIDA**. The C-H... π interaction between the selenophene and the phenyl groups of adjacent molecules is 2.85 Å, and the C-H...O hydrogen bonding interactions vary between 2.56 to 2.63 Å.

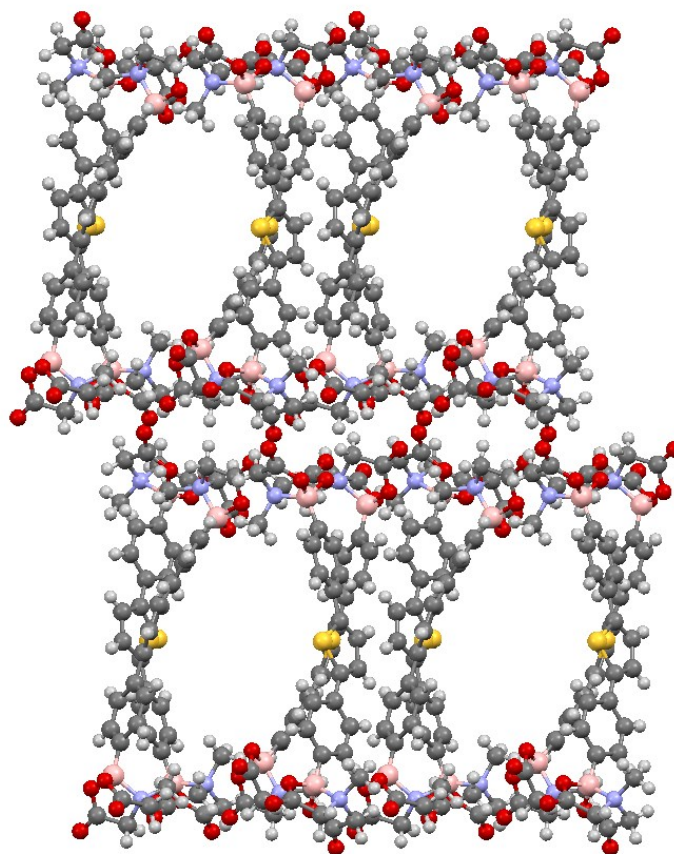


Figure S5. Microporous structure of **DPT-MIDA** view along a-axis.

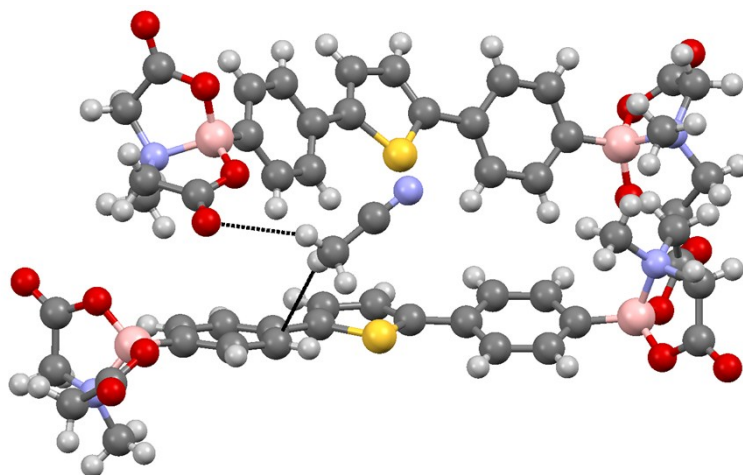


Figure S6. Interaction between guest acetonitrile molecules and **DPT-MIDA**, acetonitrile molecules without interaction are not shown.

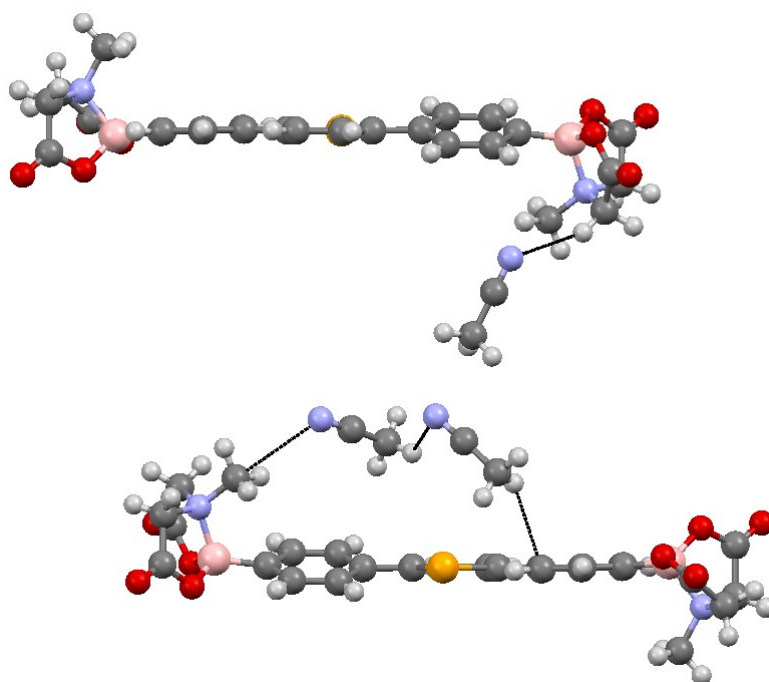


Figure S7. Interaction between guest acetonitrile molecules and **DPSe-MIDA**.

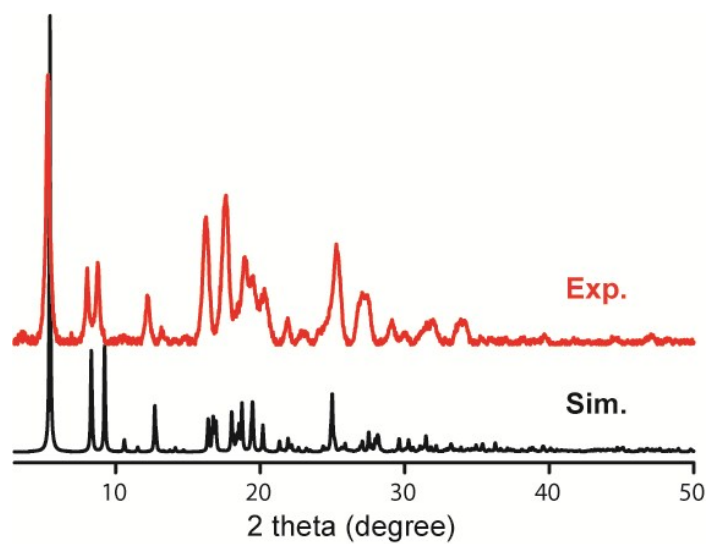


Figure S8. Experimental and simulated PXRD patterns of **DPT-MIDA**.

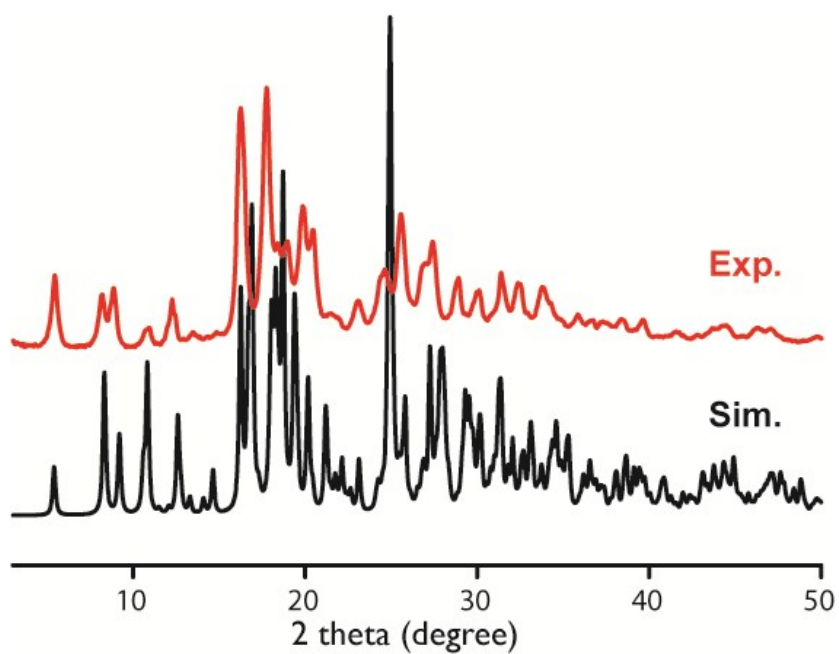


Figure S9. Experimental and simulated PXRD patterns of **DPSe-MIDA**.

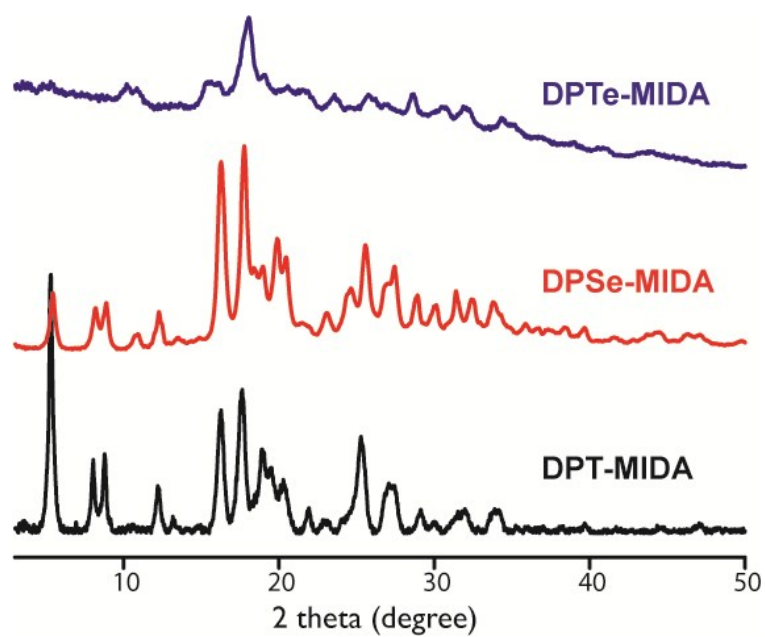


Figure S10. PXRD patterns of three frameworks.

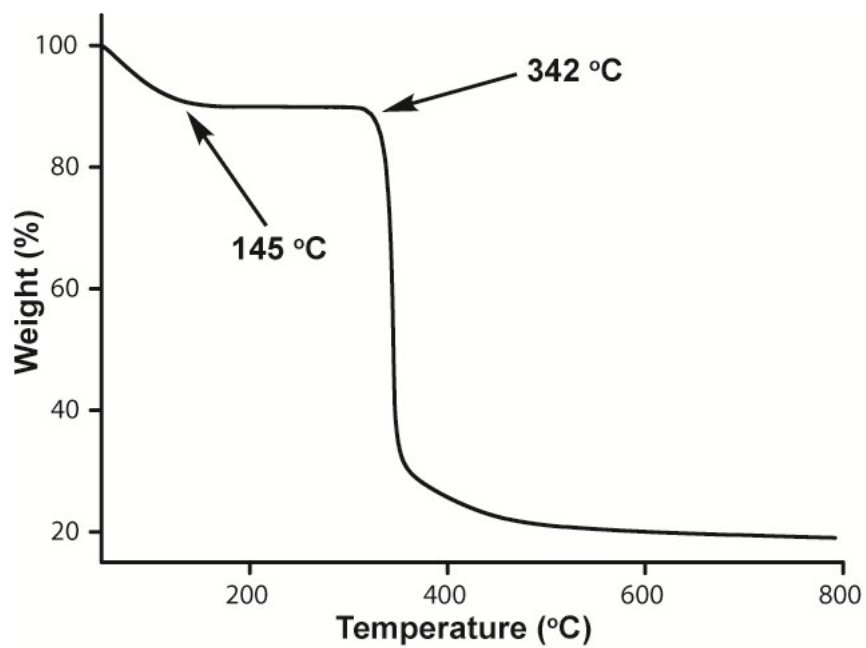


Figure S11. TGA of **DPT-MIDA** under N₂.

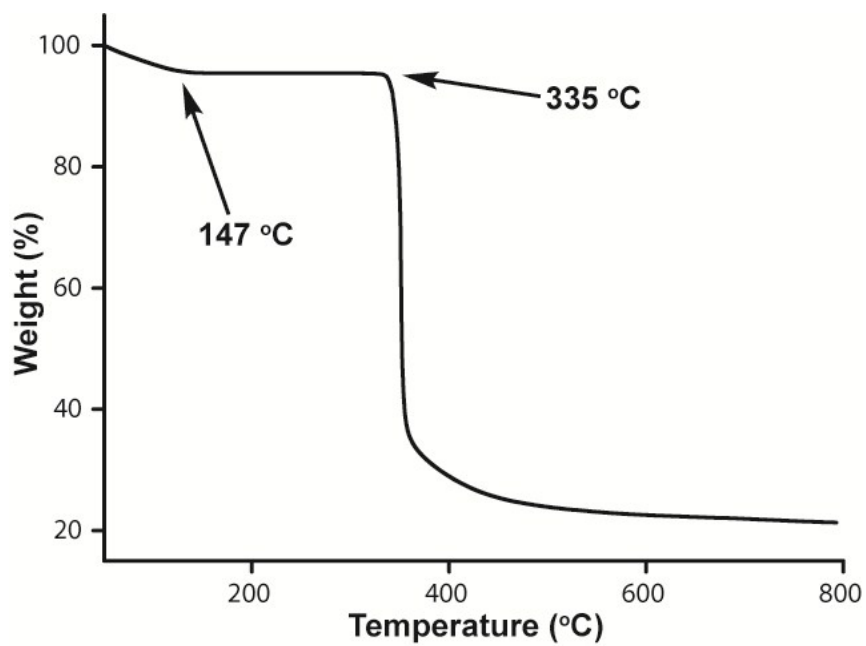


Figure S12. TGA of **DPSe-MIDA** under N₂.

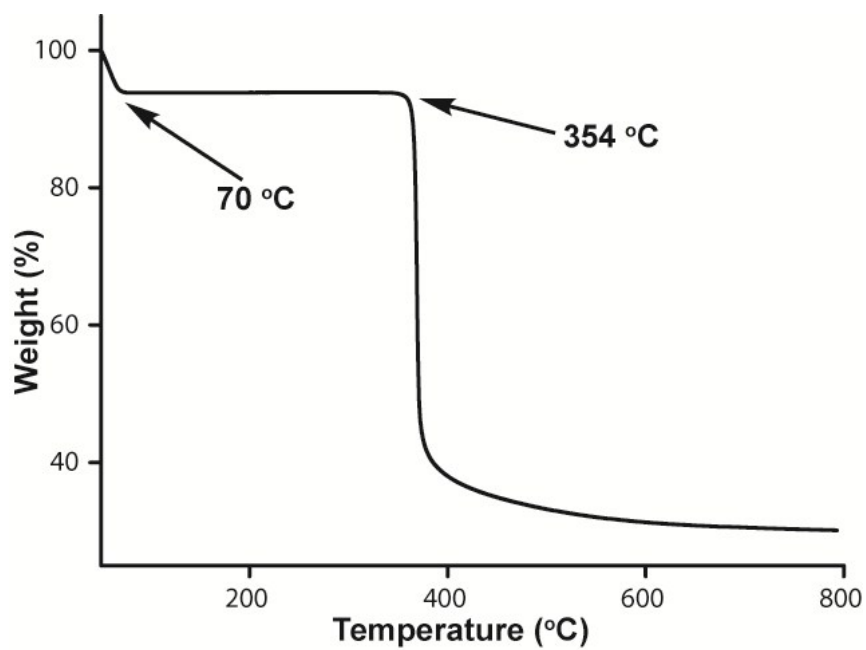


Figure S13. TGA of **DPTe-MIDA** under N₂.

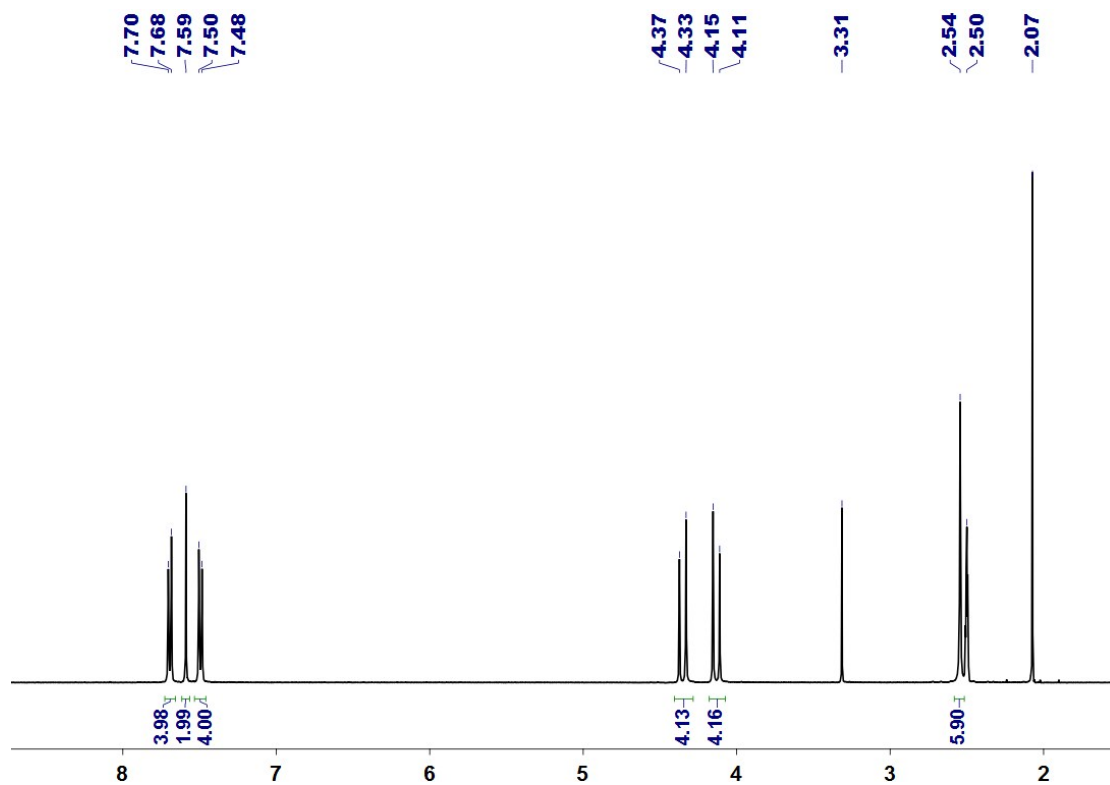


Figure S14. ^1H NMR spectrum of **DPT-MIDA** (400 MHz, $\text{DMSO-}d_6$).

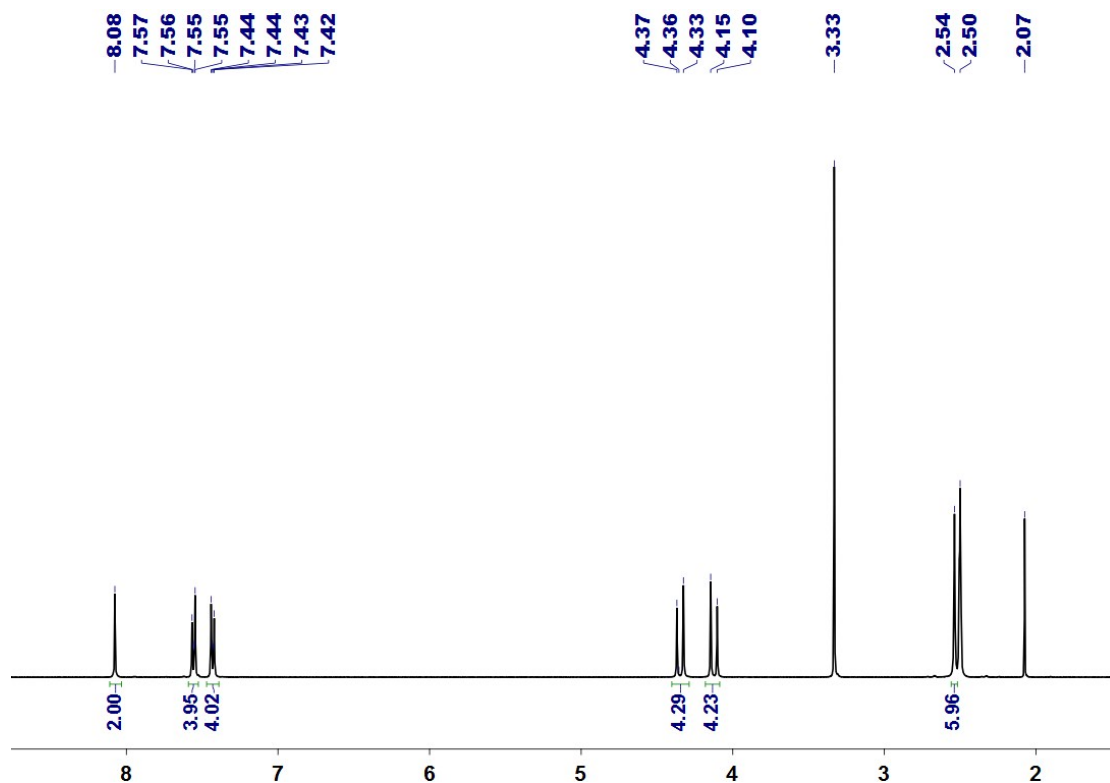


Figure S15. ^1H NMR spectrum of **DPSe-MIDA** (400 MHz, $\text{DMSO-}d_6$).



Figure S16. ^1H NMR spectrum of **DPTe-MIDA** (400 MHz, $\text{DMSO-}d_6$).

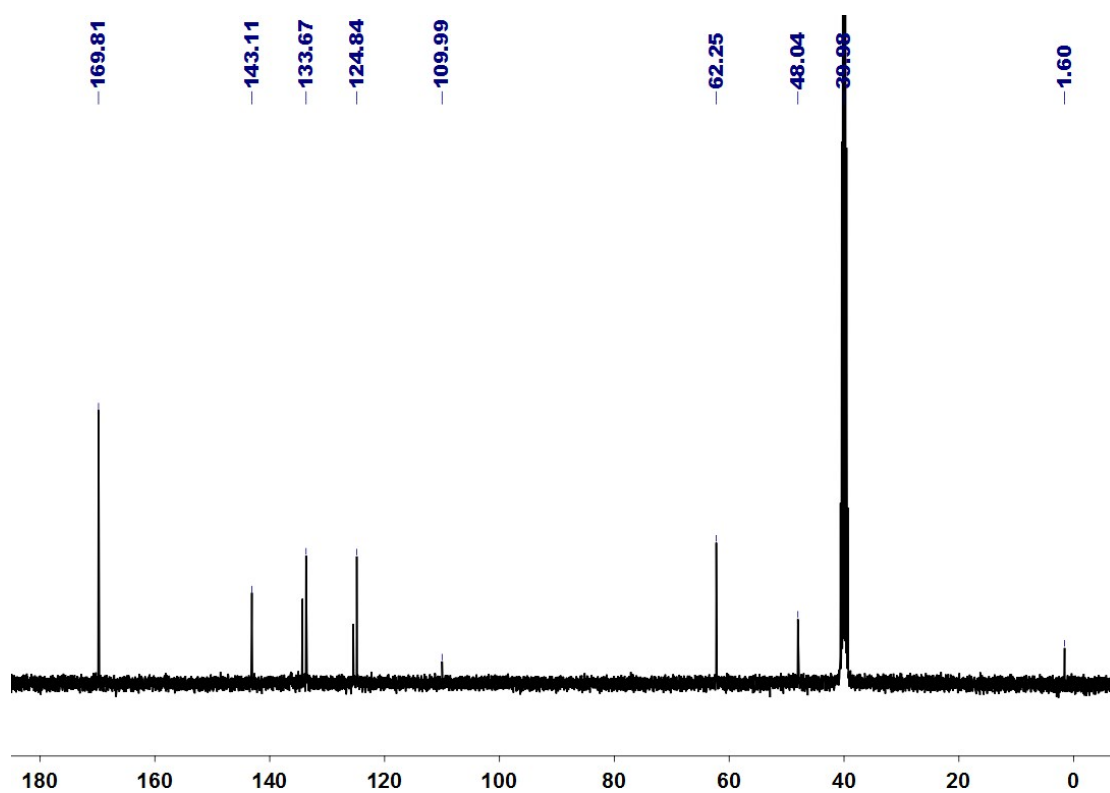


Figure S17. ^{13}C NMR spectrum of **DPT-MIDA** (100 MHz, $\text{DMSO-}d_6$).

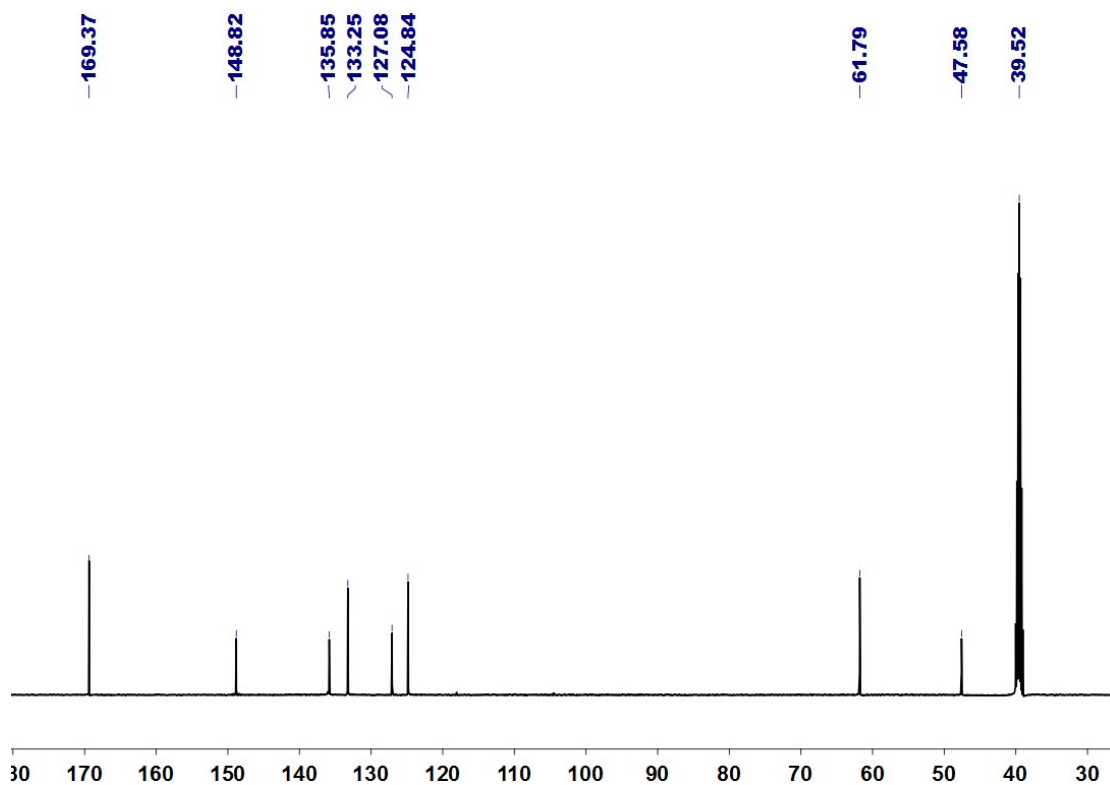


Figure S18. ^{13}C NMR spectrum of **DPSe-MIDA** (100 MHz, $\text{DMSO-}d_6$).

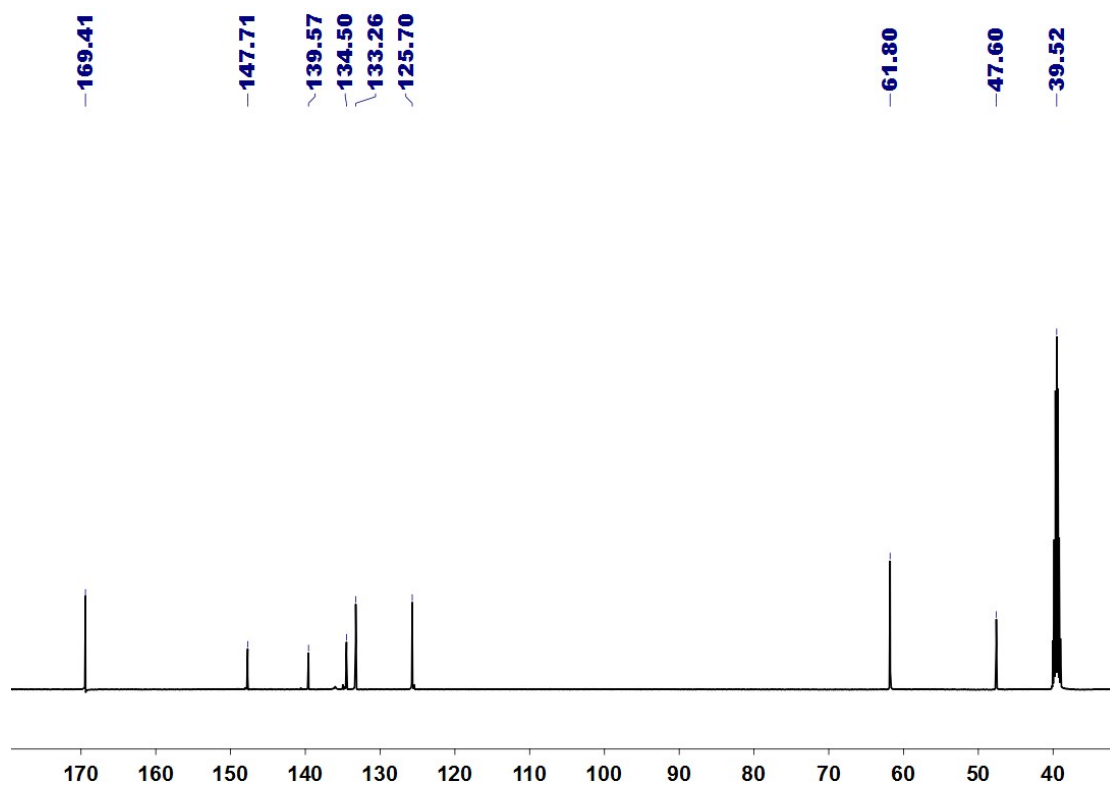


Figure S19. ^{13}C NMR spectrum of **DPTe-MIDA** (100 MHz, $\text{DMSO-}d_6$).

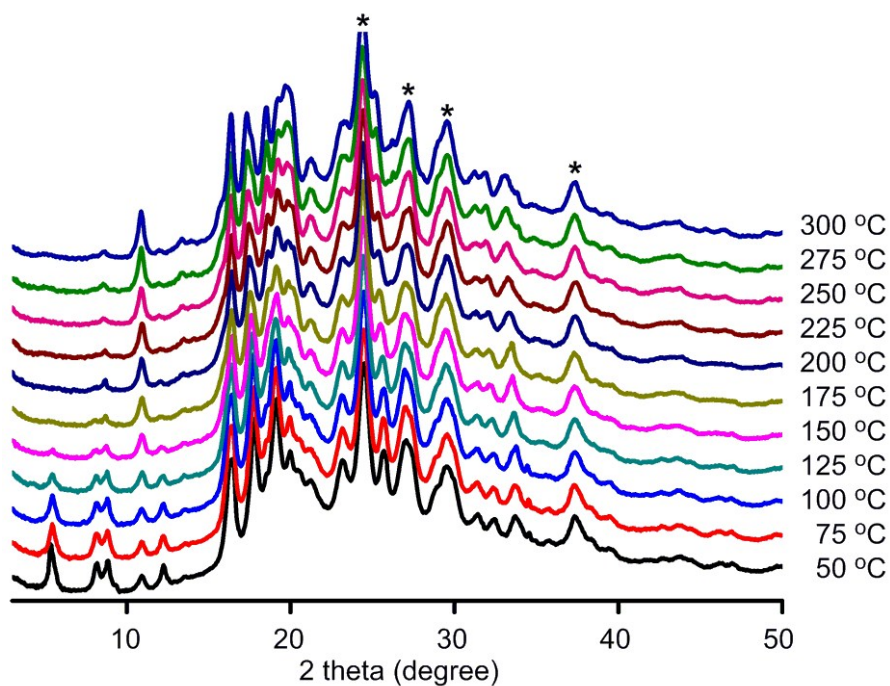


Figure S20. Variable temperature PXRD patterns of **DPSe-MIDA** under air. Asterisks (*) denotes background signal from dome.

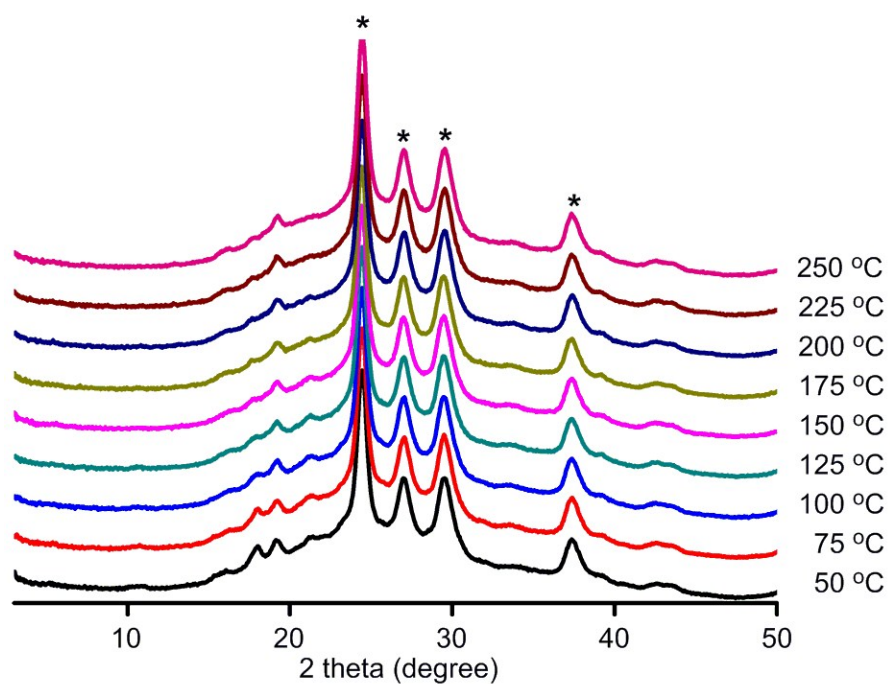


Figure S21. Variable temperature PXRD patterns of **DPTe-MIDA** under air. Asterisks (*) denotes background signal from dome.

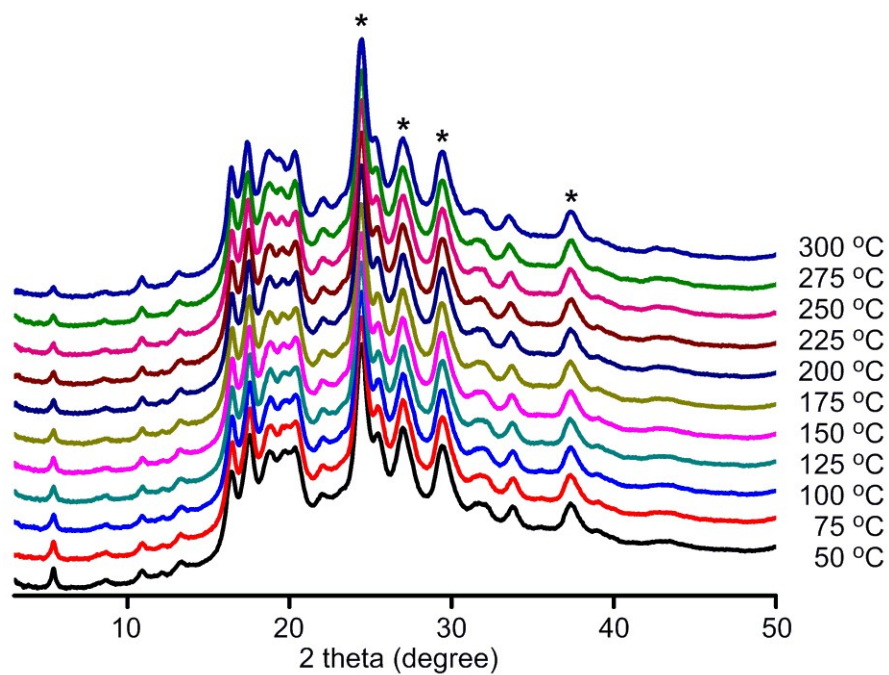


Figure S22. The variable temperature PXRD patterns of **DPT-MIDA** under vacuum. Asterisks (*) denotes background signal from dome.

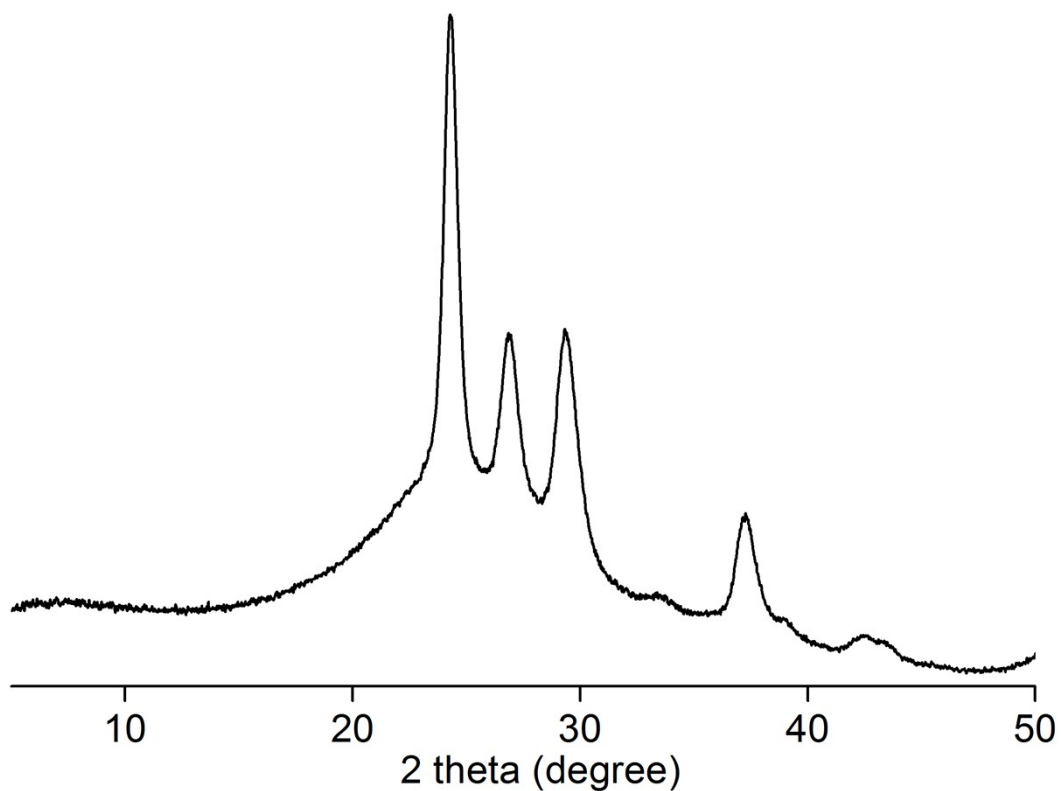


Figure S23. PXRD patterns of blank dome.

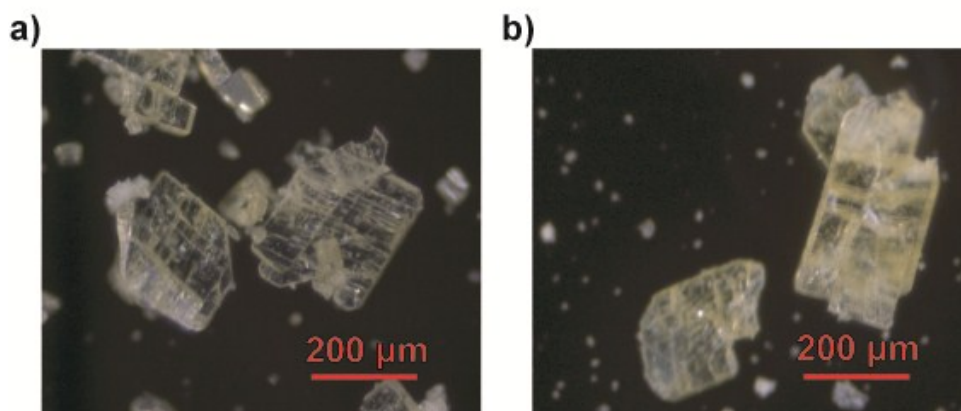


Figure S24. Optical microscope images of **DPSe-MIDA**, a) before and b) after heated at 150 °C under vacuum.

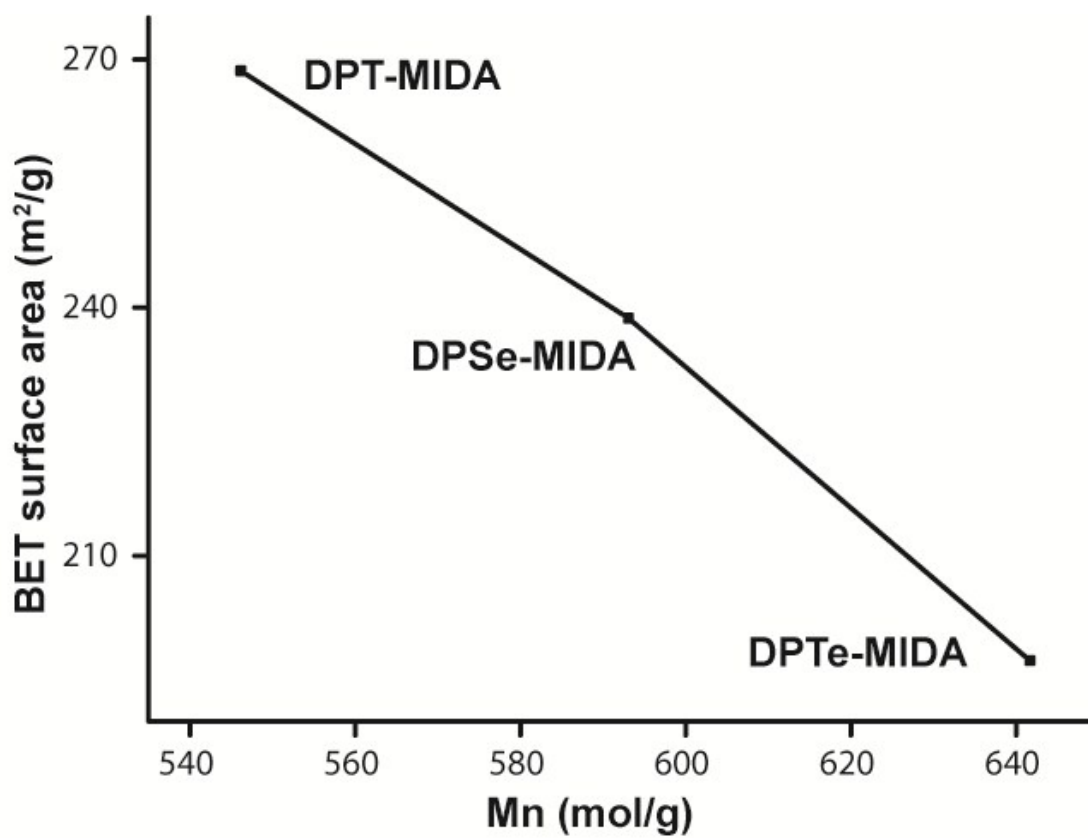


Figure S25. Linear relationship of BET surface area and Mn of **HOFs**.

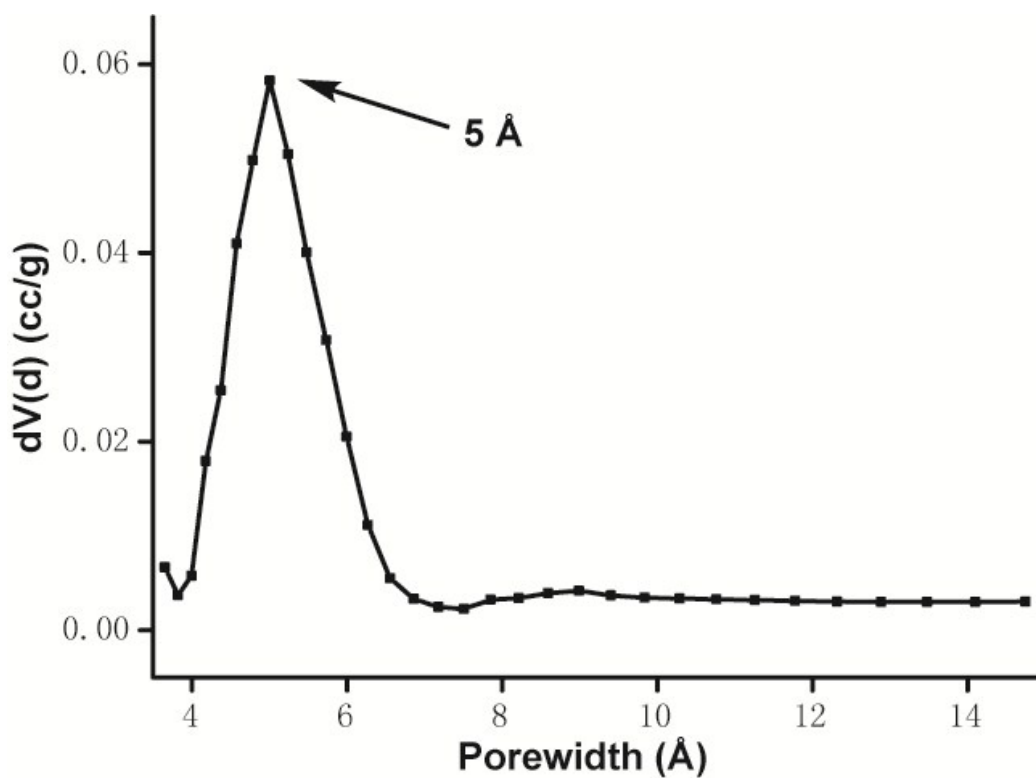


Figure S26. Pore distribution of **DPT-MIDA** by DFT method.

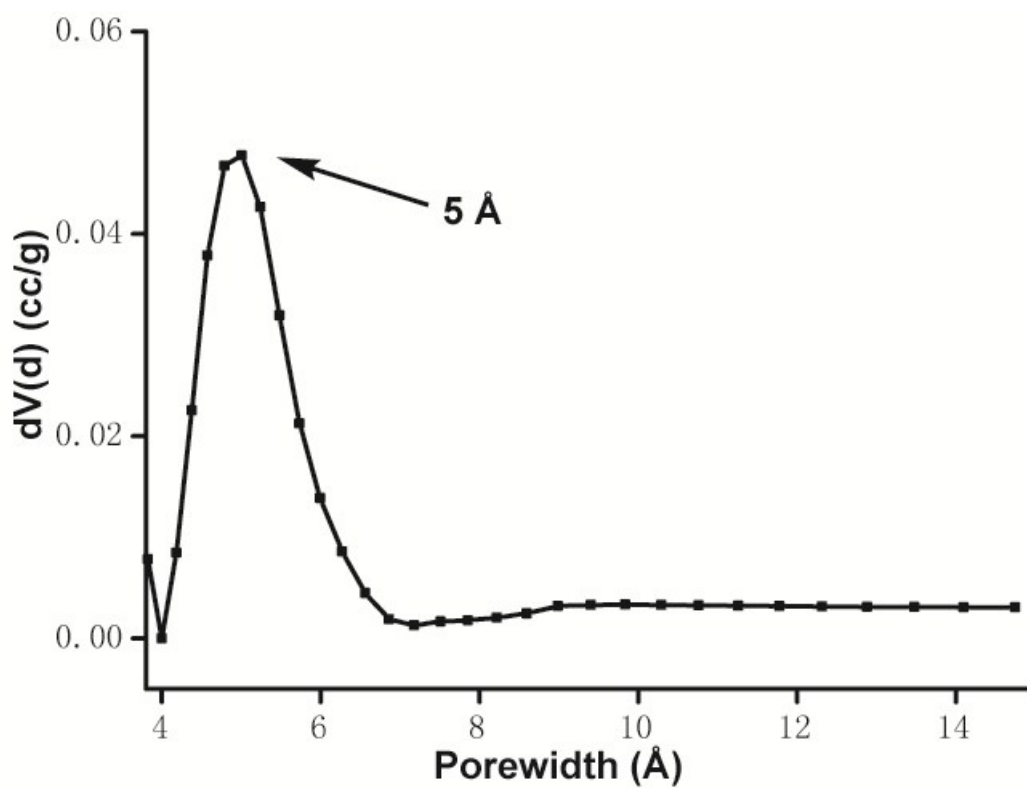


Figure S27. Pore distribution of **DPSe-MIDA** by DFT method.

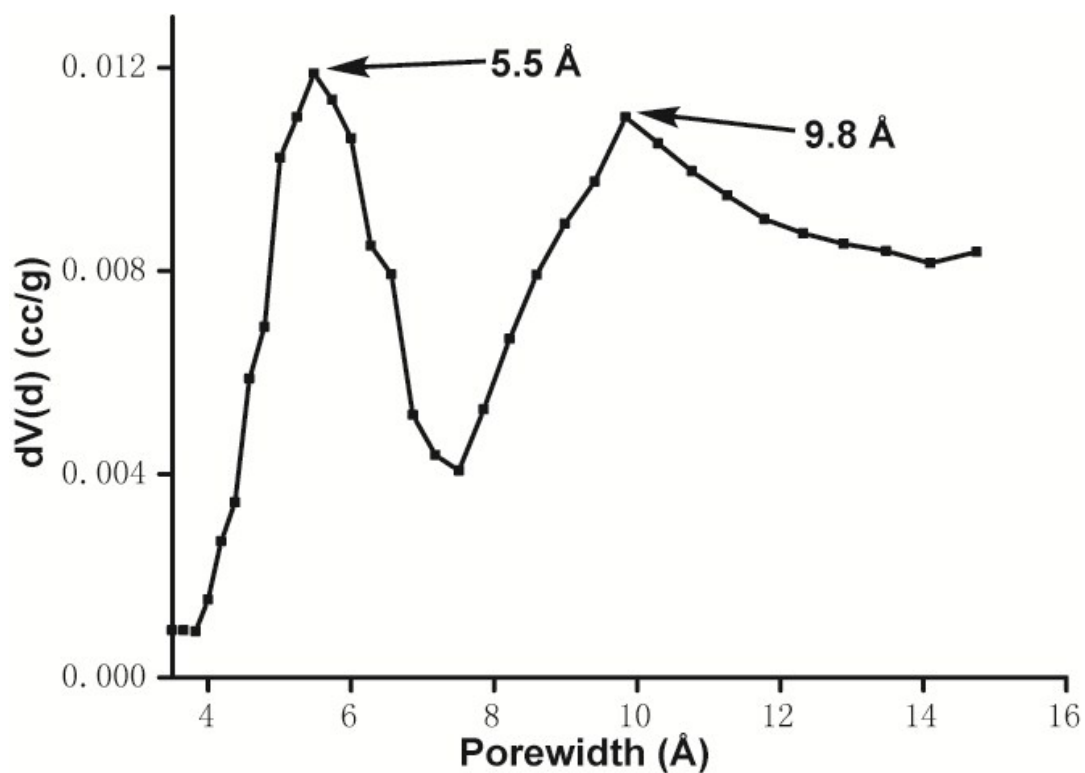


Figure S28. Pore distribution of **DPTe-MIDA** by DFT method.

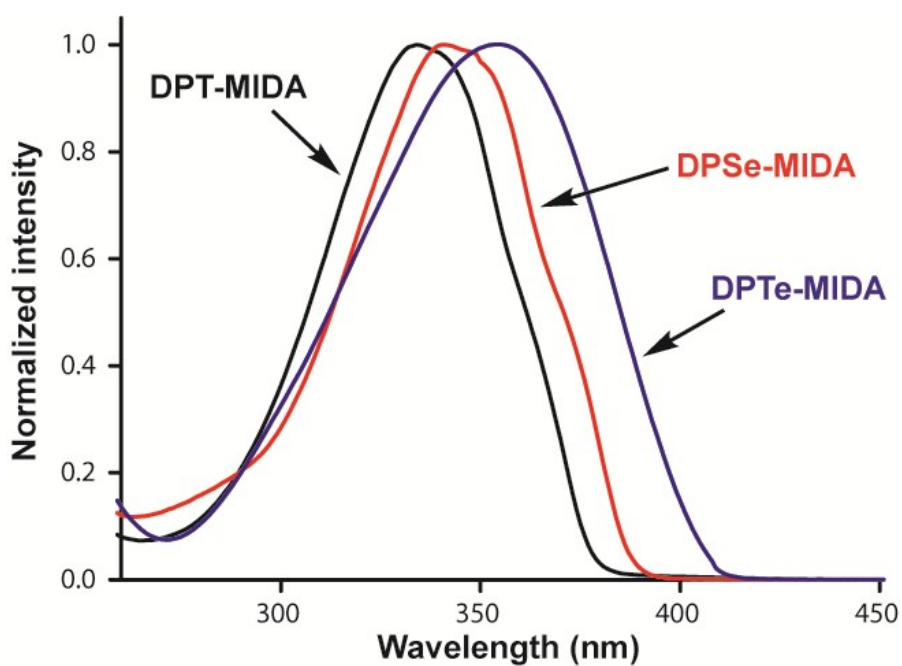


Figure S29. Normalized UV-Vis spectra of **DPT-MIDA**, **DPSe-MIDA** and **DPTe-MIDA** in acetonitrile.

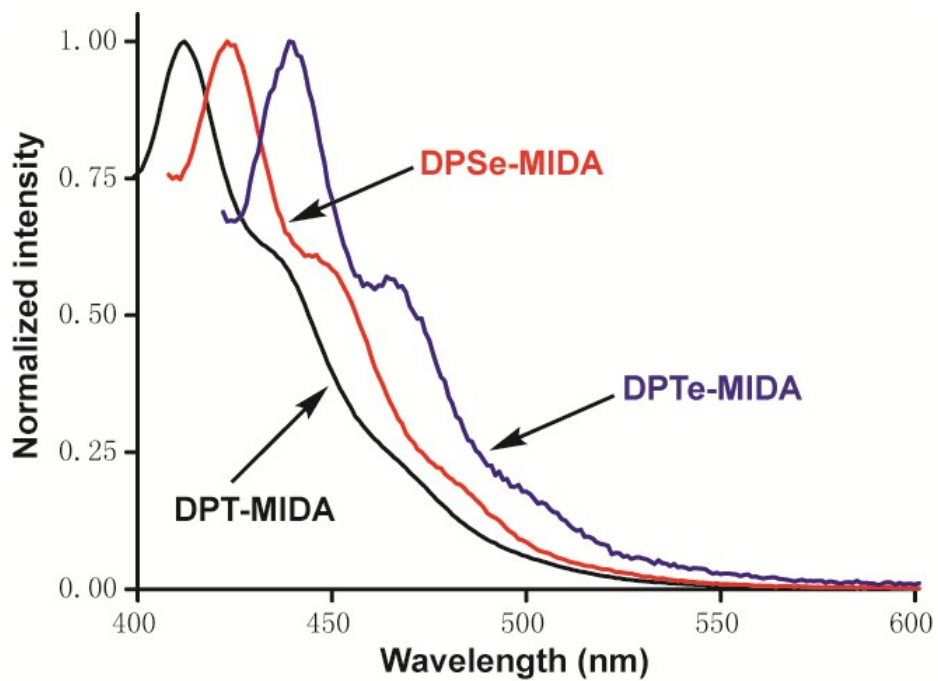


Figure S30. Normalized fluorescence spectra of **DPT-MIDA**, **DPSe-MIDA** and **DPTe-MIDA** in acetonitrile.

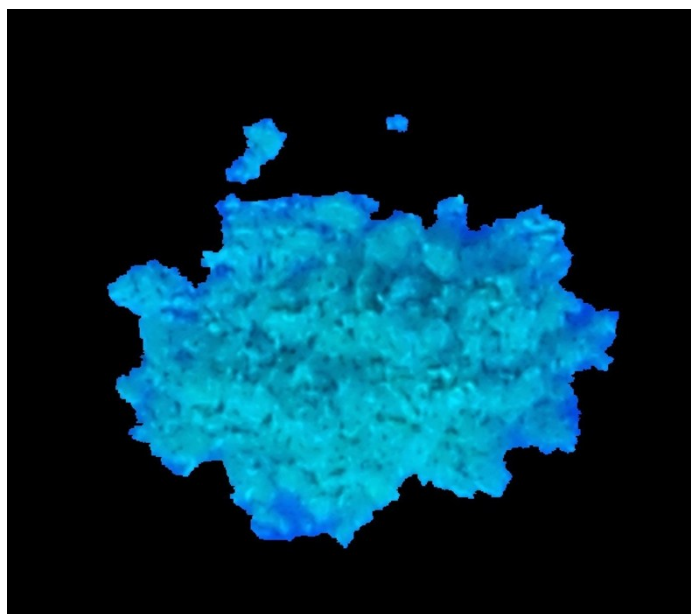


Figure S31. Image of **DPT-MIDA** powder excited by a UV lamp at 365 nm.

Table S1. Crystal data and structure refinement for **DPT-MIDA**.

Identification code	d14136_a	
Empirical formula	C ₂₉ H _{28.50} B ₂ N _{3.50} O ₈ S	
Formula weight	607.73	
Temperature	147(2) K	
Wavelength	1.54178 Å	
Crystal system	Triclinic	
Space group	P-1	
Unit cell dimensions	a = 12.3898(5) Å	α = 80.953(2)°.
	b = 12.5148(5) Å	β = 81.408(2)°.
	c = 19.2391(8) Å	γ = 85.928(2)°.
Volume	2909.5(2) Å ³	
Z	4	
Density (calculated)	1.387 Mg/m ³	
Absorption coefficient	1.473 mm ⁻¹	
F(000)	1268	
Crystal size	0.260 x 0.260 x 0.100 mm ³	
Theta range for data collection	2.349 to 67.549°.	
Index ranges	-13 ≤ h ≤ 14, -14 ≤ k ≤ 14, -22 ≤ l ≤ 22	
Reflections collected	133549	
Independent reflections	10336 [R(int) = 0.0363]	
Completeness to theta = 67.679°	98.2 %	
Absorption correction	Semi-empirical from equivalents	
Max. and min. transmission	0.7529 and 0.6495	
Refinement method	Full-matrix least-squares on F ²	
Data / restraints / parameters	10336 / 0 / 803	
Goodness-of-fit on F ²	1.030	
Final R indices [I > 2σ(I)]	R1 = 0.0353, wR2 = 0.0878	
R indices (all data)	R1 = 0.0383, wR2 = 0.0903	
Extinction coefficient	n/a	
Largest diff. peak and hole	0.251 and -0.409 e.Å ⁻³	

Table S2. Crystal data and structure refinement for **DPSe-MIDA**.

Identification code	d1522_a	
Empirical formula	C ₅₈ H ₅₇ B ₄ N ₇ O ₁₆ Se ₂	
Formula weight	1309.26	
Temperature	147(2) K	
Wavelength	0.71073 Å	
Crystal system	Triclinic	
Space group	P-1	
Unit cell dimensions	a = 12.4291(14) Å	$\alpha = 80.760(4)^\circ$.
	b = 12.5200(16) Å	$\beta = 81.900(3)^\circ$.
	c = 19.396(2) Å	$\gamma = 86.065(4)^\circ$.
Volume	2946.2(6) Å ³	
Z	2	
Density (calculated)	1.476 Mg/m ³	
Absorption coefficient	1.331 mm ⁻¹	
F(000)	1340	
Crystal size	0.210 x 0.150 x 0.025 mm ³	
Theta range for data collection	1.650 to 27.619°.	
Index ranges	-16 ≤ h ≤ 16, -16 ≤ k ≤ 16, -25 ≤ l ≤ 25	
Reflections collected	101293	
Independent reflections	13601 [R(int) = 0.0785]	
Completeness to theta = 25.242°	100.0 %	
Absorption correction	Semi-empirical from equivalents	
Max. and min. transmission	0.7456 and 0.6555	
Refinement method	Full-matrix least-squares on F ²	
Data / restraints / parameters	13601 / 0 / 791	
Goodness-of-fit on F ²	1.038	
Final R indices [I > 2σ(I)]	R1 = 0.0454, wR2 = 0.1006	
R indices (all data)	R1 = 0.0875, wR2 = 0.1153	
Extinction coefficient	n/a	
Largest diff. peak and hole	1.013 and -0.718 e.Å ⁻³	

Reference:

[1] Mangolini, L.; Jurbergs, D.; Rogojina, E.; Kortshagen, U. *J. Lumin.* 2006, **121**, 327.

[2] Faulkner, D. O.; McDowell, J. J.; Price, A. J.; Perovic, D. D.; Kherani, N. P.; Ozin, G. A. *Laser Photon. Rev.* 2012, **6**, 802.